Magnetism in hafnium dioxide

J. M. D. Coey, M. Venkatesan, P. Stamenov, C. B. Fitzgerald, and L. S. Dorneles
Physics Department, Trinity College, Dublin 2, Ireland
(Received 13 August 2004; revised manuscript received 10 November 2004; published 22 July 2005)

Thin films of HfO_2 produced by pulsed-laser deposition on sapphire, yttria-stabilized zirconia, or silicon substrates show ferromagnetic magnetization curves with little hysteresis and extrapolated Curie temperatures far in excess of 400 K. The moment does not scale with film thickness, but in terms of substrate area it is typically in the range 150–400 μ_B nm^{-2}. The magnetization exhibits a remarkable anisotropy, which depends on texture and substrate orientation. Pure HfO_2 powder develops a weak magnetic moment on heating in vacuum, which is eliminated on annealing in oxygen. Lattice defects are the likely source of the magnetism.

DOI: 10.1103/PhysRevB.72.024450 PACS number(s): 75.70.−i, 75.50.Pp, 73.20.−r

I. INTRODUCTION

We recently discovered that thin films of hafnium dioxide deposited on *R*-cut sapphire exhibit anisotropic ferromagnetic behavior at room temperature. The magnetic moment was of order 0.1 μ_B per formula unit.[1] This result was unprecedented, as magnetic order had never previously been observed in an oxide composed of ions with closed-shell configurations. The ions in question in HfO_2 are Hf^{4+} [Xe] $4f^{14}$ and O^{2-} [Ne]. We subsequently found that ZnO films doped with Sc exhibited a moment of 0.3 μ_B per scandium.[2] Again, all the ions have closed-shell configurations Sc^{3+} [Ar], Zn^{2+} [Ar] $3d^{10}$. The only comparable reports were those of a very small magnetic moment, of order $10^{-4}-10^{-2}$ μ_B per formula unit, in ceramics or crystals of CaB_6, undoped or doped with 0.5 at. % La.[3–5] The Curie temperature there was 900 K. Subsequent studies of highly pure powder showed no measurable ferromagnetism,[6] the effect was attributed to traces of iron or iron boride in the crystals.[7,8] Nonetheless, there are persistent indications of small ferromagnetic moments in CaB_6, which depend on sample stoichiometry and heat treatment.[4,6,9] We recently observed large moments in disordered thin films of CaB_6 and SrB_6.[10] Other reports of what may be called "d^0 ferromagnetism" are for certain carbon polymorphs which may contain a high concentration of defects.[11–13]

On the theoretical side, it has long been known that two-electron defect centers in oxides, such as a neutral cation vacancy (V^0 center), can have a spin triplet ground state or low-lying excited state.[14] Elfimov and co-workers[15] showed that the V^0 center in CaO produces a moment of about 2 μ_B, due to two electrons in orbitally degenerate e_g molecular orbitals, mainly associated with holes on the surrounding oxygen ions, which couple to form a $^3A_{2g}$ triplet state. A density-functional-theory calculation of a CaO supercell with a Ca vacancy indicated that these moments order ferromagnetically. Other calculations by Kenmochi and co-workers indicate a narrow, spin-split impurity band provided CaO is hole doped with B, C, or N.[16] On the basis of self-consistent GGA electronic structure calculations, Monnier and Delley suggested that a B_6 vacancy in CaB_6 induces a magnetic moment of 2.4 μ_B on next-neighbor B_6 ions, which order magnetically.[17] Our own model of exchange in dilute *n*-type ferromagnetic semiconductors mediated by donor electrons in a spin-polarized impurity band also opened the possibility of ferromagnetism in systems with a formal d^0 cation configuration.[18] Defects in insulators with wide band gaps may therefore offer a path to realize unique ferromagnetic materials.

Here our purpose is to present a detailed account of the phenomenon of d^0 ferromagnetism in HfO_2. We include data on films of different thickness prepared in different conditions on various substrates with and without cation substitution, as well as data on reduced and oxidized powders of HfO_2. The results suggest an origin associated with lattice defects in this high-*k* dielectric oxide, defects which we suspect are located near the interface with the substrate.

II. RESULTS

Three different hafnium dioxide powders used in our investigation were of nominal purity 98%, 99.95% and 99.999 %. Zirconium was the major metallic impurity identified by the suppliers and in the second and third cases all other metals together were less than 10 ppm. Our own energy dispersive x-ray (EDAX) analysis of these powders showed that indium was the main impurity in the first case (0.2 at. %); Fe, Co, and Ni were found to be below the detection limit of 0.1 wt. %.

All the thin films were prepared by pulsed-laser deposition (PLD). 13-mm disc targets were first made by sintering pressed powder in air at 1150 °C. Targets were also prepared with additions of 5 at. % Sc, Ti, or Ta; 2–10 at. % Fe; or 0.5–10 at. % Co. Films were deposited using a KrF excimer laser operating at 248 nm with an energy density of 1.8 J cm^{-2} on the target. The substrates were *R*-cut $(1\bar{1}02)$ or *C*-cut (0001) sapphire, yttria-stabilized zironia [YSZ (100)], or silicon (100) wafers treated in HF. Sapphire and YSZ substrates were typically $5\times5\times0.5$ mm^3. They were normally maintained at 750 °C during deposition, and the oxygen pressure was varied in the range 10^{-4} to 1 mbar. Some films were deposited at higher or lower temperature. Most of our films were deposited on sapphire. Neutron activation analysis of a typical sapphire substrate showed the presence of the following impurities—Mn:3 ppm; Fe: <1 ppm; Co:3–4 ppm; and Ni: <1 ppm.

Film thickness was estimated by *in situ* reflectivity monitoring, and calibrated by analysis of small-angle x-ray scat-

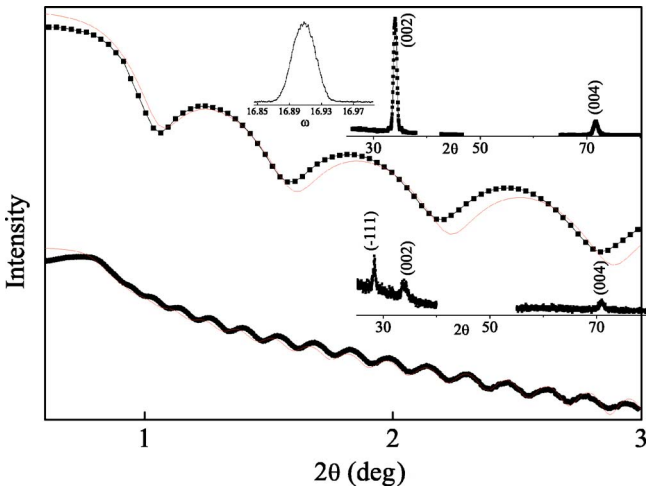

FIG. 1. (Color online) Small-angle x-ray scattering for two films of HfO_2 on *C*-cut sapphire. The upper one has a thickness of 12.7 nm; the lower one has a thickness of 51.3 nm. The diffraction peaks from the films are shown (including the region where the strongest peak of α-Fe would be seen). A rocking curve for the 002 peak of the thinner film is shown in the inset. The solid lines are simulations for uniform HfO_2 layers of the stated thickness.

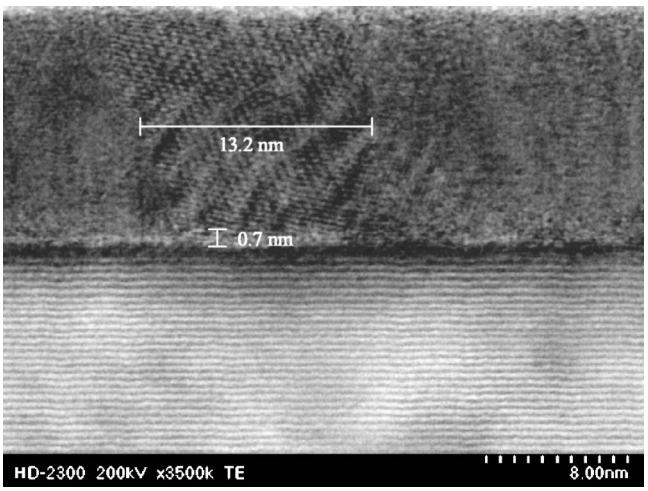

FIG. 2. Bright-field TEM lattices images of a film of HfO_2 deposited on sapphire.

tering measured on a Philips X'pert Pro diffractometer and lie in the range 0.6–400 nm. Several blank substrates were processed at the same temperature, without any laser deposition, as a control. Films are transparent and colorless. The optical absorption edge was at 5.9 eV as expected for HfO_2. Films appeared smooth and featureless in the scanning electron microscope (SEM), with few of the droplets often seen in films produced by PLD. When examined in the SEM or AFM, some of the films showed shallow depressions on the surface typically 2–5 μm in diameter. X-ray data for two films of different thickness are shown in Fig. 1. Roughness deduced from the fits to the small-angle scattering data was less than 0.2 nm for a 15-nm film. The two sharp peaks for the thinner film are tentatively identified as the 002 and 004 reflections of the monoclinic HfO_2 structure with $c=0.533$ nm, assuming $\beta=99.1°$.[19] A rocking curve of the 002 reflection gives a full width at half maximum of 0.04°, which is the instrumental resolution. The thicker film shows a $(\bar{1}11)$ reflection as well, indicating a more random texture.

Different textures are observed on the other substrates, or even on the same substrate in different conditions. For instance, a film deposited in 1-mbar oxygen pressure showed reflections which could be indexed on the tetragonal HfO_2 structure, whereas those on *R*-cut sapphire had a monoclinic (002) texture and those on silicon exhibited reflections of the monoclinic HfO_2 structure with no clear orientation. Hafnium dioxide has several structural polymorphs, so it is impossible to be sure which one is present from the few x-ray reflections exhibited by an oriented film.

Figure 2 shows a TEM image of a cross section of a film on sapphire which has a columnar texture with column diameter ~8 nm. The lattice image of the interface region shows a fine grained (~10 nm) polycrystalline texture. Analytical nanoprobe investigations showed that any concentrations of Fe, Co, or Ni in the films were insignificant; the *M*:Hf ratio was less than the detection limit, 0.1 wt. %. Ferromagnetic impurities in the film at this level could account for no more than 1% of the observed moments. The images were obtained in an Hitachi 2300 scanning transmission electron microscope.

The masses of the sapphire substrate were in the range 43–48 mg and their area was 23 mm^2. The film masses were of order 10 μg. Samples were mounted in straws for magnetization measurements with the substrate either horizontal (perpendicular to the applied field) or vertical (parallel to the applied field). Typical room-temperature data measured in a 5-T quantum design MPMS XL superconducting quantum interference device (SQUID) magnetometer are presented in Fig. 3. The first curve shows the diamagnetism of a blank sapphire substrate subjected to the same thermal cycle in the deposition chamber as one with a thin film deposited on it. The susceptibility -4.8×10^{-9} $m^3\,kg^{-1}$ agrees with the accepted value for sapphire, -4.6×10^{-9} $m^3\,kg^{-1}$.

The SQUID measurements were all made using a standard second-order gradiometer, around the maximum slope position of the second derivative curve, with no autotracking of the actual sample position. Generally the magnetization of each film was measured both with the field perpendicular and parallel to the substrate. The SQUID is calibrated for a sample occupying a volume of diameter 3 mm and height 3 mm at the center of the pickup coils. The substrates extend beyond this region and the sensitivity of the instrument is modified by an amount that depends on the sample orientation. In order to obtain accurate data on the anisotropy of the magnetic moment, we calculated the response of the coils to a 5×5 mm^2 film, which was assumed to be uniformly magnetized, and oriented perpendicular or parallel to the applied field. The response was 19% smaller in the latter case. The calculation was confirmed experimentally by measuring films of cobalt and magnetite in both directions.

The second panel in Fig. 3 shows data for an HfO_2 film on *R*-cut sapphire. The ferromagnetic signal remaining after subtraction of the linear diamagnetic background is shown in the third panel. The background slope is defined by data in the range 3–5 T. This procedure for reducing the data yields

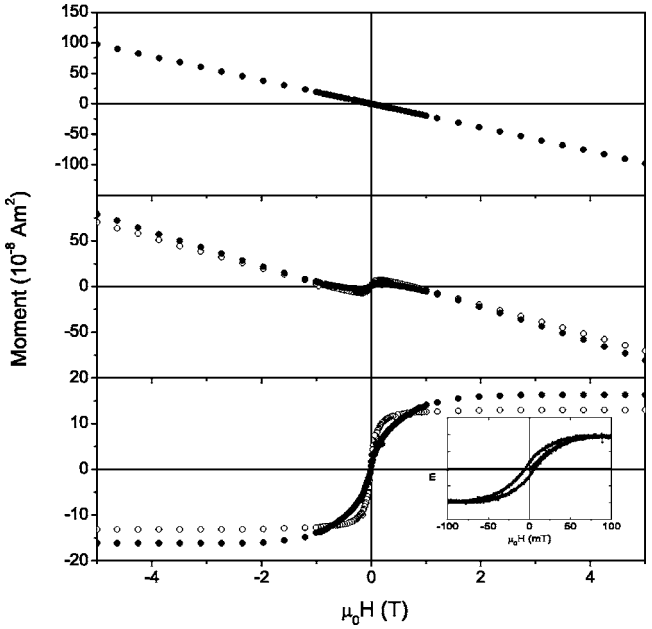

FIG. 3. Room-temperature magnetization curves of (a) a blank sapphire substrate, (b) the substrate with an 82-nm film of HfO_2, and (c) data for the HfO_2 film after subtracting the background diamagnetism of the substrate. (●) Perpendicular to substrate, (○) parallel to substrate.

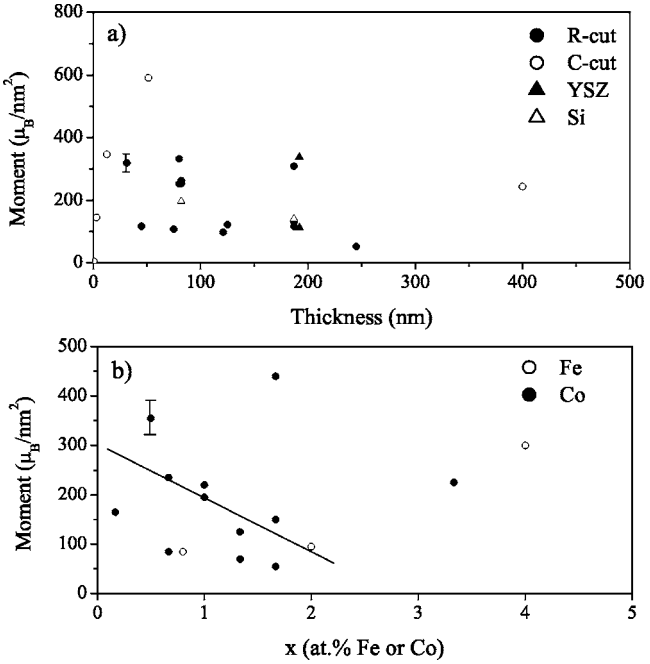

FIG. 4. Room-temperature magnetic moments of HfO_2 films deposited at 10 Hz on different substrates (a) undoped, as a function of thickness and (b) Co or Fe doped, as a function of concentration.

accurate values for the ferromagnetic moment, but does not provide the high-field slope for fields greater than 3 T.

The diamagnetic susceptibility of HfO_2 was measured on an 80-mg sintered pellet made from 99.95% pure powder. The room-temperature value is -1.6×10^{-9} m^3 kg^{-1}. Because of their relative masses, the diamagnetic signal from the substrate is three orders of magnitude greater than the diamagnetic signal of the thin film deposited on it. Hence the diamagnetism of the HfO_2 films is not measurable.

Table I summarizes typical data obtained for HfO_2 films deposited from different targets in different circumstances. Forty-two pure and doped films have been measured, some of them repeatedly. Films were usually measured within one month of deposition. Only in the very thinnest film ($\approx$0.6 nm) was no magnetic moment observed at room temperature. The data on undoped HfO_2 in Fig. 4(a) shows that the moment does not depend in any simple way on the thickness of the film. All moments for undoped films on *R*-cut sapphire or silicon are in the range $26-81\times10^{-9}$ Am^2, grown from any of the targets. The moments on *C*-cut sapphire tend to be somewhat larger. The moment per unit substrate area usually lies in the range 150–400 μ_B nm^{-2}. The scatter of the data points exceeds the experimental error in deducing the magnetization, which is represented by a typical error bar in the figure. The moment of films made from

TABLE I. Magnetic properties of HfO_2 films deposited in different conditions. Moments are measured at room temperature. Errors in thickness are ±5%. The errors of the measurement of σ are 5×10^{-9} Am^2.

No.	Composition	Substrate	Thickness (nm)	$\sigma_\perp$(10^{-9} Am^2)	$\sigma_\parallel$(10^{-9} Am^2)	σ_{av}(10^{-9} Am^2)
1	HfO_2	*R*-Al_2O_3	80	108	27	81
2	HfO_2	*R*-Al_2O_3	82	90	36	72
3	HfO_2	*R*-Al_2O_3	31	73	65	70
4	HfO_2	Si	187	27	32	29
5	HfO_2	YSZ	192	64	76	68
6	HfO_2	*C*-Al_2O_3	13	345	292	327
7	HfO_2	*C*-Al_2O_3	13	83	70	78
8	HfO_2	*C*-Al_2O_3	51	140	120	133
9	$Hf_{0.94}Sc_{0.06}O_2$	*R*-Al_2O_3	~90	11		11
10	$Hf_{0.97}Ti_{0.03}O_2$	*R*-Al_2O_3	~90	12		12
11	$Hf_{0.80}Ta_{0.20}O_2$	*R*-Al_2O_3	~90	10		10
12	$Hf_{0.98}Fe_{0.02}O_2$	YSZ	~90	19	27	22
13	$Hf_{0.98}Co_{0.02}O_2$	YSZ	~80	88	118	98

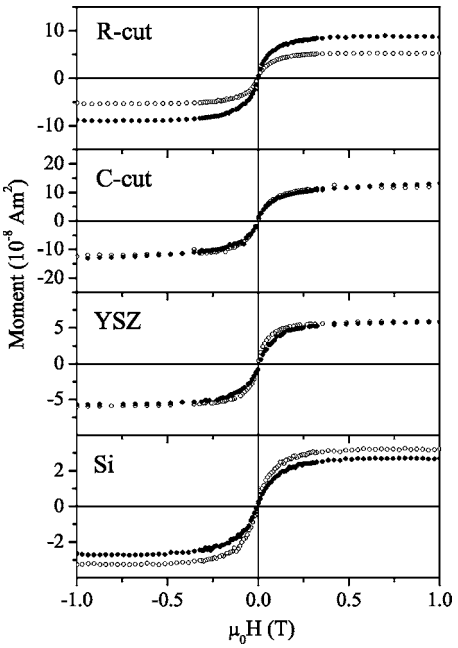

FIG. 5. Anisotropic magnetization of HfO_2 films deposited on different substrates. (●) Perpendicular to substrate, (○) parallel to substrate.

the same target in the same conditions are reproducible to within about 20%. An error analysis of all the data in Fig. 4(a) gives a mean value of 236 μ_B nm^{-2} with a standard deviation of 181 μ_B nm^{-2}. The probability that the moment is nonzero at the 99% confidence limit is >99.8%. The data in Fig. 4(a) are statistically inconsistent with proportionality of moment and film thickness.

That the magnetic moment is really associated with the HfO_2 film was demonstrated in one case where the HfO_2 grown on a *C*-cut sapphire substrate was removed by argon-ion milling. The moment then fell from 140×10^{-9} Am^{-2} to less than 5×10^{-9} Am^{-2}.

The films show coercivity of 2–5 mT at room temperature and remanence of 2–5 % of saturation. The detail of a hysteresis loop measured using an alternating gradient force magnetometer is included as an inset in Fig. 3(c). Hysteresis at 5 K is similar to that at room temperature.

The magnetization of the HfO_2 films is practically temperature independent, at least up to 400 K. Saturation magnetization values differ by less than 5% between 5 and 400 K.[1] Complete magnetization curves were measured at fixed temperatures, with the sample being recentered to allow for the effect of thermal expansion of the support on the sample position. The data was reduced as described above. The extrapolated Curie temperatures were therefore far in excess of 400 K.

The magnetization of the films is remarkably anisotropic. Figure 5 compares data for films deposited on four different substrates. There it is seen that the magnitude of the moment can vary by as much as a factor of 2, and the sign of the anisotropy depends on the substrate and hence on the crystallographic texture of the HfO_2. The anisotropy cannot be explained in terms of the sensitivity of the SQUID pickup coils, which is ~19% less when the film is vertical than when it is horizontal. The anisotropy of the saturation magnetization effectively rules out an explanation of the magnetization in terms of any known segregated ferromagnetic impurity in the films.

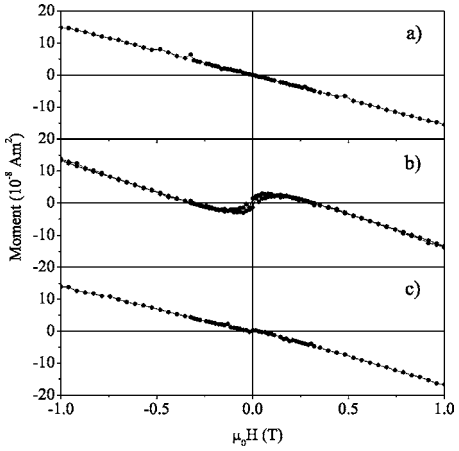

FIG. 6. Room-temperature magnetization curves of HfO_2 powder measured (a) as received, (b) after heating at 750 °C in vacuum, and (c) after reheating the same sample at 750 °C in air.

The moments were unstable over extended periods of time. Samples remeasured after about six months showed moments that were less than 10% of those measured originally.

Doping appears to reduce the moment of films. This is true for Sc, Ti, or Ta, but also for Co and Fe, at least at low levels. The trend for Co is suggested in Fig. 4(b). The cobalt-doped films with more than 1 at. % Co begin to exhibit appreciable coercivity, for example 23 mT for the 3% Co doping. The moment expressed per Co ion is 30 μ_B at the lowest cobalt doping (0.5%). However, there is no reason to associate the large moment exclusively with cobalt, as the moment of undoped films of the same thickness can be just as high, if not higher. The magnetization in Co- or Fe-doped HfO_2 therefore consists of a component from the transition-metal ion not expected to exceed its spin-only value, and a component such as that in the undoped films which is thought to originate from lattice defects. The data suggest that the two components are oppositely aligned in the dilute limit.

In order to test for a defect-related origin of the ferromagnetism, we have examined the influence of reduction and oxidation on the magnetism of the pure HfO_2 powder. The as-received powder is diamagnetic. After heating at 750 °C for 2 h in vacuum, it develops a small ferromagnetic signal, corresponding to a moment $\sigma=1.9\times10^{-3}$ Am^2 kg^{-1} or 7×10^{-5} μ_B per formula unit. This moment can be eliminated by reheating the powder at 750 °C for 30 min in air, as shown in Fig. 6. The main defects introduced by heating hafnia in vacuum are likely to be oxygen vacancies.[19] Assuming a moment of order 1 μ_B per defect, the vacancy concentration in the reduced powder is 70 ppm. Given the powder particle size of approximately 1 μm, concentration of these defects at the 0.1% level would place them in a surface shell 12-nm thick, which is comparable to the thickness of the thin films we have prepared.

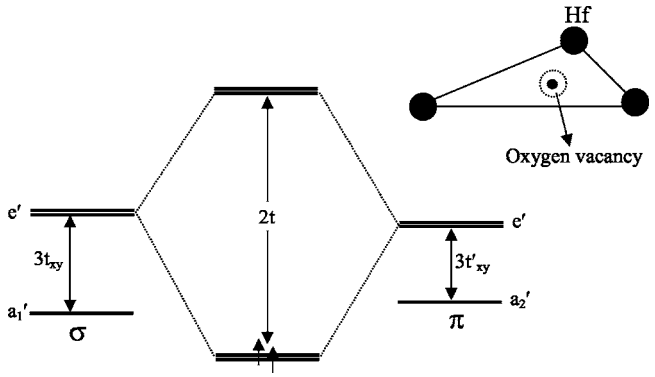

FIG. 7. Formation of molecular orbitals around an oxygen vacancy in HfO_2 coordinated by three hafnium ions.

III. DISCUSSION

The lack of proportionality of magnetic moment and film thickness indicates an origin at the film surface or the interface with the substrate, rather than in the bulk. The difference in the initial slope of the magnetization curves measured parallel or perpendicular to the plane of some films suggests an anisotropy field of 0.2–0.5 T [Fig. 3(c)]. Attributing this to shape anisotropy of an interface layer, the thickness of this ferromagnetic layer is approximately 5–15 nm.

Interfacial defects on silicon have been studied in the context of using HfO_2 as a high-k dielectric layer.[20] In that case, besides the tendency of the HfO_2 to form oxygen vacancies, there is formation of a silicate interface layer.

One way in which magnetic moments could arise from atomic point defects in HfO_2 is as follows. Monoclinic HfO_2 contains oxygen sites that are surrounded by three or four hafnium ions. Taking a neutral three-coordinated oxygen vacancy with D_{3h} symmetry, for example, molecular orbitals are formed from the valence electrons on the three hafnium ions surrounding the vacancy. These have σ or π symmetry with respect to the Hf–[O] bond axis, where [O] represents the vacant oxygen site. From the σ orbitals, with a Hf–Hf transfer integral t_{xy}, a_1', and e' orbitals are formed at energy $\varepsilon-2t_{xy}$ and $\varepsilon+t_{xy}$, respectively. Similarly, for the π orbitals with transfer integrals t'_{xy} and t_z orbitals of a_2', e', a_2'', and e'' symmetry are formed at $\varepsilon-2t'_{xy}$, $\varepsilon+t'_{xy}$, $\varepsilon-2t'_z$, and $\varepsilon+t'_z$, respectively. Only the σ and π orbitals of e' symmetry will mix, giving bonding and antibonding states with a splitting $2t$, as shown in Fig. 7. Provided $t>t'_{xy}$, it is possible for the ring of charge orbital formed from the e' orbitals to be stabilized relative to the symmetric a_1 state. Furthermore, since the orbital is degenerate, it can accept two electrons of the same spin, giving a spin moment of 2 μ_B. The ring may also possess an orbital moment, and spin-orbit coupling is expected to be important for hafnium. The large anisotropy of the moment is then attributed to the orientation of the charge rings relative to the interface plane.

Hafnium vacancies are less likely than oxygen vacancies on account of their high charge state, but if they do occur in significant amounts, at grain boundaries for example, the holes created on the surrounding oxygen ions will be highly correlated, with a much stronger tendency than electrons to form high-spin molecular orbital states.[15] Hunds rule coupling for oxygen is ~2.0 eV. Recent density functional theory calculations by Pemmaraju and Sanvito[21] have shown that the hafnium vacancy is the only defect which creates a robust, stable moment. The moment of magnitude $4\mu_B$ is distributed over the surrounding oxygen. They find strong ferromagnetic coupling of the defects on first and second-neighbor sites. What may be required is a mechanism by which oxygen vacancies can produce oxygen holes. The high charge of the Hf^{4+} ion tends to polarize the surrounding $2p^6$ oxygen shells, an effect which may be enhanced by the asymmetry created by an oxygen vacancy in the vicinity. The polar state is represented by promotion of the $2p$ oxygen electron to a $3s$ state. The $2p$ holes then tend to form molecular orbitals with parallel spins on account of the oxygen Hunds rule coupling.

These defect-related molecular orbitals may be rather extended in view of the fairly large optical dielectric constant of hafnium dioxide ($\varepsilon\approx5$). When present in sufficient concentration, the defect-related orbitals will form an impurity band, which will be insulating provided their concentration is not too high.[18] Direct exchange between the molecular orbitals will be ferromagnetic and may be strong when the defects are concentrated in an interface layer. The moments of order 200 μ_B nm^{-2} indicate that the defect concentrations in thin (~10 nm) films are of order 10%. Detailed application of an impurity band model to HfO_2 requires a knowledge of the defect states at the interface, and appropriate electronic structure calculations, but such a model could account, at least qualitatively, for the paradoxical d^0 ferromagnetism in this material.

IV. CONCLUSIONS

The present results suggest an alternate focus for the search for ferromagnetic semiconductors and insulators–oxides with d^0 cations in a high charge state. There may be no need to substitute magnetic cations into certain nonmagnetic matrices in order to make them ferromagnetic. In the case of HfO_2, where magnetic cations are not detected, it seems it is sufficient to have the right kind of defects. The nature of these defects should be revealed by further comparative studies of films produced by PLD, or other techniques such as sputtering or chemical vapor deposition, which have greatly different magnetic moments. When the nature of the defects and their electronic structure has been elucidated in HfO_2, it should become clearer why the phenomenon is not more widespread.

The defect-related magnetism is remarkably different from any previously known room-temperature ferromagnetism in that it is highly anisotropic. This allows us to eliminate trace amounts of secondary phases of iron or magnetite, for example, as a direct explanation of the phenomenon. It is a challenge to explain the huge anisotropy together with a near absence of hysteresis, which may reflect the presence of persistent orbital currents due to unpaired electrons in extended molecular orbitals associated with the defects.

ACKNOWLEDGMENTS

This work was supported by the Science Foundation of Ireland. We are grateful to Professor James Lunney for the

use of his Pulsed Laser Deposition facilities, and to M. Kamino and Yang Zhou for the TEM and AGFM measurements, respectively. We have benefited from useful comments from G. A. Sawatzky and N. Krasnikova. L. S. Dorneles was supported by the Irish Research Council for Science, Engineering and Technology (IRCSET).

[1] M. Venkatesan, C. B. Fitzgerald, and J. M.D. Coey, Nature (London) **430**, 630 (2004).
[2] M. Venkatesan, C. B. Fitzgerald, J. G. Lunney, and J. M. D. Coey, Phys. Rev. Lett. **93**, 177206 (2004).
[3] D. P. Young, D. Hall, M. E. Torelli, Z. Fisk *et al.*, Nature (London) **397**, 412 (1999).
[4] T. Terashima, C. Terakura, Y. Umeda, N. Kimura, H. Aoki, and S. Kunii, J. Phys. Soc. Jpn. **69**, 2423 (2000).
[5] P. Vonlanthen, E. Felder, L. Degiorgi, H. R. Ott *et al.*, Phys. Rev. B **62**, 10 076 (2000).
[6] B. K. Cho, J. S. Rhyee, B. H. Oh, M. H. Jung *et al.*, Phys. Rev. B **69**, 113202 (2004).
[7] M. C. Bennett, J. van Lierop, E. M. Berkeley, J. F. Mansfield *et al.*, Phys. Rev. B **69**, 132407 (2004).
[8] K. Matsubayashi, M. Maki, T. Tsuzuki, T. Nishioka, and N. K. Sato, Nature (London) **420**, 143 (2002).
[9] S. E. Lofland, B. Seaman, K. V. Ramanujachary, N. Hur, and S. W. Cheong, Phys. Rev. B **67**, 020410(R) (2003).
[10] L. S. Dorneles, M. Venkatesan, M. Moliner, J. G. Lunney, and J. M. D. Coey, Appl. Phys. Lett. **85**, 6377 (2004).
[11] T. L. Makarova, B. Sundqvist, R. Höhne, P. Esquinazi *et al.*, Nature (London) **413**, 716 (2001).
[12] P. Esquinazi, D. Spemann, R. Höhne, A. Setzer *et al.*, Phys. Rev. Lett. **91**, 227201 (2003).
[13] T. L. Makarova, Semiconductors **38**, 615 (2004).
[14] A. M. Stoneham, *Theory of Defects in Solids* (Clarendon, Oxford, New York, 1975), Ch. 16.
[15] I. S. Elfimov, S. Yunoki, and G. A. Sawatzky, Phys. Rev. Lett. **89**, 216403 (2002).
[16] K. Kenmochi, M. Seike, K. Sato, A. Yanase, and H. Katayama-Yoshida, Jpn. J. Appl. Phys., Part 2 **43**, L934 (2004).
[17] R. Monnier and B. Delley, Phys. Rev. Lett. **87**, 157204 (2001).
[18] J. M.D. Coey, M. Venkatesan, and C. B. Fitzgerald, Nat. Mater. **4**, 173 (2005).
[19] A. S. Foster, F. Lopez-Gejo, A. L. Shluger, and R. M. Nieminen, Phys. Rev. B **65**, 174117 (2002).
[20] A. I. Kingon, J. P. Maria, and S. K. Streiffer, Nature (London) **406**, 1032 (2000).
[21] C. D. Pemmaraju and S. Sanvito, Phys. Rev. Lett. **94**, 217205 (2005).